journal

J. Am. Ceram. Soc., **89** [7] 2226–2231 (2006)
DOI: 10.1111/j.1551-2916.2006.00996.x

Microstructural Modifications in Macroporous Oxides Prepared Via Latex Templating: Synthesis and Thermal Stability of Porous Microstructure

Carla Verissimo[†] and Oswaldo L. Alves

LQES-Laboratório de Química do Estado Sólido, Instituto de Química, Universidade Estadual de Campinas,
UNICAMP, 13084-971 Campinas, SP, Brazil

Titanium and zirconium oxides with interconnected macropores presenting well-defined pore sizes and controlled three-dimensional ordering were prepared using a latex templating method. Polystyrene spheres were used as pore templates, whereas metal alkoxides were used as oxide precursors. The final thermal treatment at different temperatures showed macroporous microstructure stabilities up to 600°C. At higher temperatures, a collapse of the macroporous microstructure and sintering were observed, as well as phase transformations in the oxides structures during the calcination process, as shown by Raman spectroscopy and X-ray diffraction techniques.

I. Introduction

Ceramic macroporous materials with pore sizes between 50 nm and 10 μm, a narrow diameter distribution, and three-dimensional ordering of pores can present very interesting properties, leading to several applications such as in separation processes, catalysis, adsorbents, insulators, lightweight structural materials, and low dielectric constant materials.[1–4] Moreover, macroporous materials can also present unusual optical properties, permitting preparation of optical devices like photonic crystals with optical bandgaps.[1–8] However, until recently, there has been no general method available for producing such materials.[1,2] In the last few years, a new approach using colloidal crystals as self-assembled templates for macropores has been used to prepare macroporous materials with well-defined pore sizes and controlled three-dimensional ordering.[1–4,6–19]

Colloidal crystals can be considered as monodisperse particles self-assembled to form an ordered three-dimensional array. These artificial opals, as they are known, obtained from emulsion droplets or latex spheres, have been used as pore templates with appropriate dimensions for the preparation of ceramic macroporous materials, as shown by Imhof and Pine[1,12] Velev *et al.*,[2] Holland *et al.*,[3,11] Wijnhoven and Voss[4] and other authors.[6–10,13–19]

The emulsion templating method requires several efforts in the preparation of monodisperse droplets, employing a tedious fractionation procedure.[20] Moreover, the latex spheres present lower values of polydispersity when compared with emulsion droplets and larger domain sizes of well-ordered spheres.[21] In general, the use of colloidal crystals prepared from latex spheres has been an easier and more versatile method to obtain these macroporous matrices.

The idea of this experimental approach is to use monodisperse particles such as self-assembled latex spheres to form an ordered three-dimensional array. A precursor solution of the desired final solid is added to the template and it infiltrates into voids between the latex spheres. Wet chemistry techniques such as the sol–gel process are then used to prepare the macroporous solid material, so that it captures the self-organization from the colloidal crystals via solidification of the continuous medium by a sol–gel transition. The template can be removed by calcination leading to a macroporous structure. In most cases, a final thermal treatment is necessary not just to eliminate the organic template but also to produce a solid having a desired crystalline phase. This stage is very important as the macroporous microstructure associated with a specific crystalline phase can provide the properties of the material leading to its final application.

In this paper, macroporous titanium oxide (TiO_2) and zirconium oxide (ZrO_2) were prepared using latex spheres as pore templates, and the influence of the thermal treatment temperature on the stability of the macroporous microstructure as well as the phase transformations during the calcination process are reported.

II. Experimental Procedures

(1) Materials

All chemicals were used without further purification. The chemicals used were titanium tetraisopropoxide (97%, Sigma-Aldrich, St. Louis, MO), zirconium *n*-propoxide (23%–28% free alcohol, Strem Chemical, Inc., Newburyport, MA), and 2,4-pentanedione (>99,5%, Merck, Whitehouse Station, NJ). A monodisperse polystyrene sphere suspension (380 nm diameter, 10 wt%) was ordered from Bangs Laboratories Inc. (Fishers, IN).

(2) Preparation of Macroporous TiO_2 and ZrO_2

An aqueous suspension (0.3 mL) of 380 nm polystyrene spheres (10 wt%) was centrifuged at 3000 rpm for 3 h and dried under vacuum for 5 h to form latex macrocrystals, further used as a macropore template.

TiO_2 was prepared using titanium tetraisopropoxide treated with two equivalents of chelating agent 2,4-pentanedione and diluted in 1:1 v/v isopropanol. Later, 0.1 mL of this solution was added dropwise to the latex macrocrystal previously placed over an absorbent surface. TiO_2 was also prepared by the direct addition of pure titanium tetraisopropoxide onto the latex macrocrystal kept inside the centrifuge tube.

ZrO_2 was prepared using zirconium *n*-propoxide diluted in 1:1 v/v isopropanol. This solution was added dropwise to the latex macrocrystals previously placed over an absorbent surface.

After permeation of oxide precursor solutions into the voids between the polystyrene spheres and solidification into an inorganic network upon drying under atmospheric conditions for 24 h, the samples were thermally treated at 600°, 800°, or 1000°C in air.

G. Franks—contributing editor

Manuscript No. 20991. Received September 13, 2005; approved January 26, 2006.
This work was financially supported by the FAPESP, under Grant No. 99/06491-7, and Millennium Institute for Complex Materials (PADCT/CNPq).
Presented at the Royal Society of Chemistry Materials Forum: Materials Discussion 5—Porous Materials and Molecular Intercalation, Madrid, Spain, September 2002 (Winner of the prize for Best Poster).
Based on the thesis submitted by C. Verissimo for the Ph.D. degree in chemistry, Campinas State University, Campinas, SP, Brazil, 2003.

[†] Author to whom correspondence should be addressed. e-mail: carla@iqm.unicamp.br

(3) Materials Characterization

Microstructure characterizations were performed by Raman spectroscopy (model System 3000 Raman Imaging Microscope, Renishaw, New Mills, UK) using the 632.8 nm line of a He–Ne laser, and scanning electron microscopy (SEM; models JSM 6360LV and JSM 6340F, JEOL, Tokyo, Japan). SEM samples were placed over an adhesive conductive carbon tape attached to a metal stub and were coated with carbon and Au/Pd films, respectively. Powder X-ray diffraction patterns (XRD) were carried out at the XRD beamline of the Brazilian Synchrotron Light Laboratory (LNLS, Campinas, Brazil) using a Si(111) double crystal to monochromatize the incident X-ray beam ($\lambda = 1.5405$ Å), at room temperature. Powder samples were filled into a thin-walled glass capillary (7 μm) with 1 mm diameter.

III. Results and Discussion

(1) Latex Macrocrystal

Different methods have been used to organize the latex spheres into three-dimensional arrays, such as sedimentation, filtration, and centrifugation. In this work, latex macrocrystals were prepared by three-dimensional ordering of polystyrene spheres using centrifugation. This process led to iridescent sediments on the bottom of the centrifuge tubes that were dried under vacuum before use.

SEM images from latex macrocrystals showed high ordering degree of polystyrene spheres after the centrifugation process. The presence of domains separated by boundaries caused by packing failures was also observed, as well as the formation of domains with different packing: hexagonal (H) and tetragonal (T) (Fig. 1(A)). The presence of hexagonal packing—each sphere surrounded by six other spheres in the same plane—suggest two different structures for the latex crystallization since hexagonal packing can be related to the face-centered cubic (fcc) structure (111) plane and hcp structure (001) plane. The tetragonal array also observed in the latex macrocrystal is related to the fcc structure (100) plane, indicating that the latex sphere packing resulted in a fcc structure (Fig. 1(B)).[11,22,23] The fcc array has been observed in several works where latex or silica spheres were three dimensionally ordered, and computer simulations have suggested that the fcc array is more stable than the hcp array.[11,22] The co-existence of both fcc and hcp arrays has also been observed in latex macrocrystals, in addition to a bcc array under specific conditions.[11,23]

Latex macrocrystals were used as macropore templates to prepare macroporous titanium and zirconium oxides, as *ca.* 74% of the volume was occupied by latex spheres and 26% was available to be filled by inorganic precursor solutions.

(2) Macroporous Oxides

Different experimental approaches were used to prepare macroporous oxides via the latex templating method, as shown in the literature.[2–4,6–11,13–19] In this work, latex macrocrystals were embedded in alkoxide precursor solutions using different procedures, as described in the experimental section.

Initially, pure titanium tetraisopropoxide was added dropwise inside the centrifuge tube containing the ordered latex spheres (latex macrocrystal). A porous oxide was not obtained by this procedure after thermal treatment at 600°C for 8 h, as observed by SEM images (figure not shown). The absence of pores in this TiO_2 sample is probably related to the high reactivity of pure titanium tetraisopropoxide, which prevented its permeation through the latex macrocrystal by capillary forces before hydrolysis.

To decrease its reactivity, titanium alkoxide was treated with the chelating agent 2,4-pentanedione. In this approach, a small volume of the chelated titanium tetraisopropoxide solution was added dropwise onto latex macrocrystal pieces previously placed over an absorbent surface. The idea was to promote the permeation of small volumes of the precursor solution through the latex macrocrystal, with the excess solution being absorbed by the surface. Scanning electron micrographs obtained after the infiltration of the alkoxide solution inside the latex macrocrystal voids showed maintenance of polystyrene sphere ordering (Fig. 2(A)). The sample was then thermally treated at 600°C for 8 h, and the SEM image shows the hexagonal packing of the latex spheres replicated in the pore arrangement of the inorganic material (Fig. 2(B)). A high three-dimensional organization of the macroporosity and a narrow distribution of pore diameters (ranging from 150–170 nm, indicating a shrinkage of 55%–60%) could be observed. The solid microstructure thus obtained constituted interconnected macropores in a well-ordered hexagonal arrangement (Fig. 2(C)).

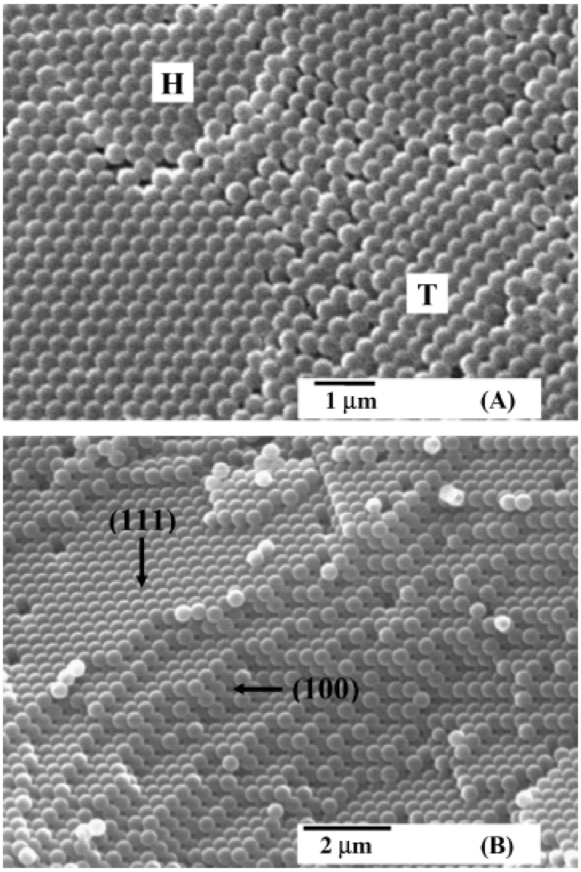

Fig. 1. Scanning electron microscopy images of the latex macrocrystal: (A) high ordering of polystyrene spheres: different domains with hexagonal (H) and tetragonal (T) packing; (B) a surface fracture presenting (111) and (001) planes of the face centered cubic structure.

When a latex macrocrystal/oxide precursor nanocomposite was formed, the drying process was started with solvent evaporation. Alkoxide hydrolysis was also taking place because of the natural humidity of air and the precursor condenses, leading to solidification of the material into an inorganic network around the template. During the thermal treatment, the latex spheres decomposed and a densification of the solid was observed, caused by condensation of the hydroxyl groups, forming an oxide network that resulted in a shrinkage of the pore diameters when compared with the polystyrene sphere size. Usually, shrinkages around 17%–35% have been reported in the literature,[3,6,7,11,15,16] which indicates that the special conditions in our experiments led to greater shrinkage. The chelation process allowed alkoxide penetration inside the latex macrocrystal structure, so as to preserve the three-dimensional ordering of the latex spheres before hydrolysis, leading to macroporous TiO_2.

ZrO_2 was also prepared by using the procedure described above. Scanning electron micrographs of latex macrocrystal obtained after the permeation of the alkoxide solution showed the

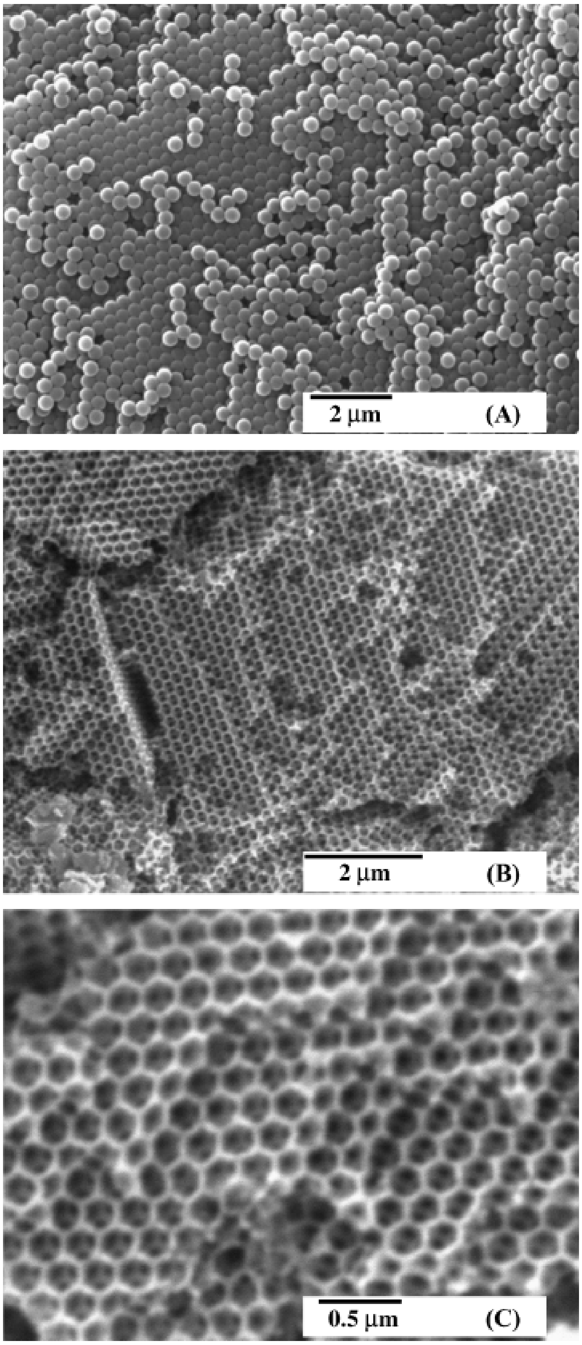

Fig. 2. Scanning electron microscopy images: (A) latex macrocrystal/titanium oxide (TiO_2) precursor nanocomposite before the thermal treatment. (B) and (C) TiO_2 sample prepared by adding the titanium alkoxide solution onto latex macrocrystal pieces placed over an absorbent surface after the calcination at 600°C for 8 h in air.

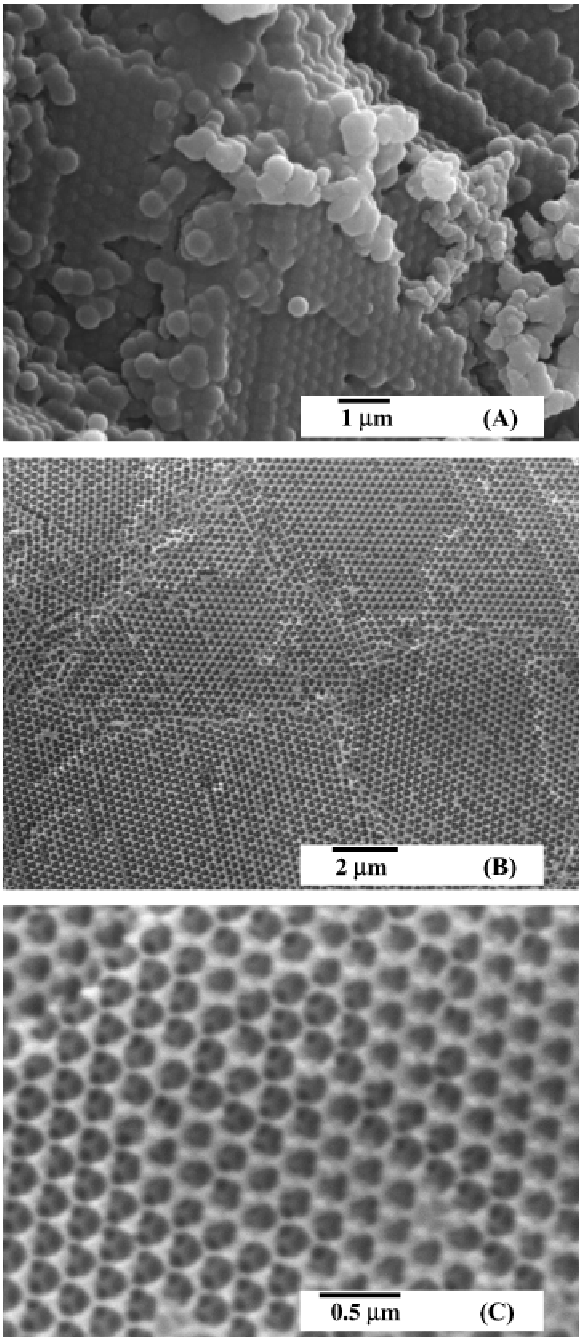

Fig. 3. Scanning electron microscopy images: (A) latex macrocrystal/zirconium oxide (ZrO_2) precursor nanocomposite before the thermal treatment; (B) and (C) micrographs at different magnifications of the macroporous ZrO_2 obtained after the calcination at 600°C for 8 h in air.

preservation of sphere ordering and a visible coating formed by the initial hydrolysis of the ZrO_2 precursor (Fig. 3(A)). After thermal treatment at 600°C for 8 h, the SEM image showed large domains with a high pore organization (Figs. 3(B) and (C)). As observed previously for TiO_2 samples, ZrO_2 material also presented interconnected macropores with diameters between 160 and 190 nm that demonstrated a narrow distribution and shrinkage around 50%–60%.

SEM images allowed the visualization of the oxide microstructure constituted by interconnected macropores in a well-ordered hexagonal arrangement–as shown by Figs. 2(C) and 3(C)–and the evaluation of the different experimental procedures to obtain macroporous templated ceramic solids.

The thermal stability of the macroporous microstructures was investigated by thermal treatment of the oxide samples at temperatures higher than 600°C. For TiO_2 treated at 800°C for 1 h, SEM micrographs showed domains with different microstructures (Fig. 4). Figure 4(A) shows the loss of pore organization, the beginning of macroporous microstructure disruption, with the cracking of pore walls, as indicated by arrows, and TiO_2 sphere growth. In the same sample, some regions were constituted only by TiO_2 spheres, as shown in Fig. 4(B). A pattern in the disposition of TiO_2 spheres was observed, indicating a hexagonal distribution of these spheres. Taking into account the slightly hexagonal shape of the pores, as observed in Fig. 2(C), TiO_2 spheres were formed in the vertices of the pores. Sintering of the TiO_2 spheres was also observed, as shown in Fig. 4(C), which led to agglomeration and neck formation. In the case of thermal treatment at 1000°C for 1 h (Fig. 5), the macroporous microstructure was completely damaged and microparticles pre-

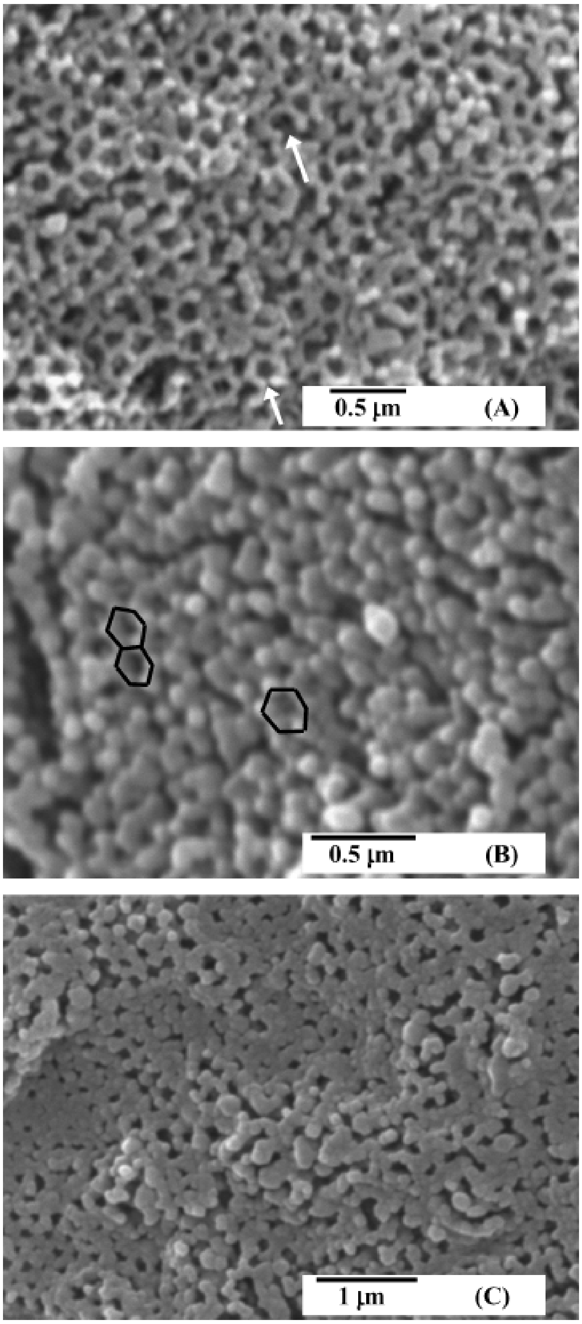

Fig. 4. Scanning electron microscopy images of the titanium oxide (TiO_2) thermally treated at 800°C showing a disruption of the macroporous microstructure: (A) crack of pore walls (arrows); (B) TiO_2 sphere growth; (C) sintering.

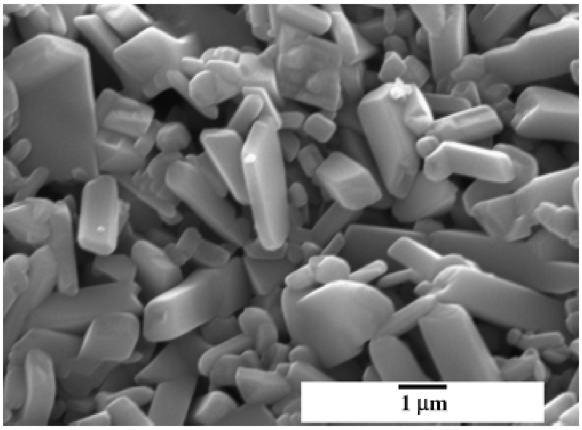

Fig. 5. Scanning electron microscopy image of the titanium oxide thermally treated at 1000°C.

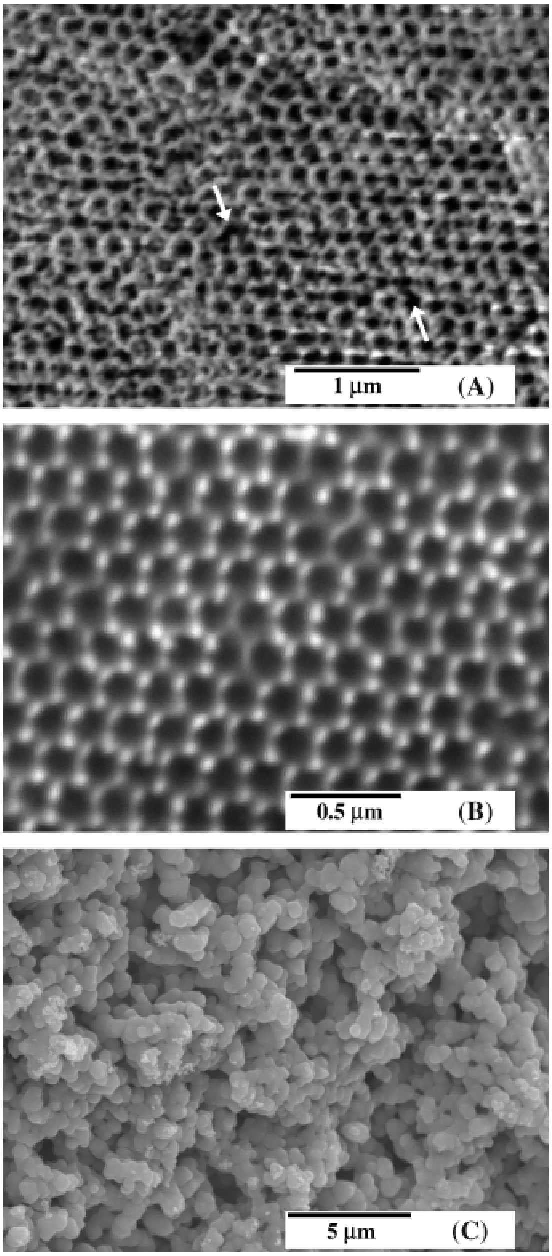

Fig. 6. Scanning electron microscopy images of the zirconium oxide (ZrO_2) thermally treated at 800°C showing a disruption of the macroporous microstructure: (A) crack of pore walls (arrows); (B) ZrO_2 sphere growth; (C) sintering.

sented geometric shapes and sizes between 0.1 and 2.5 µm. ZrO_2 samples treated at 800° and 1000°C exhibited the same behavior as observed for the TiO_2 (Fig. 6).

According to our results, thermal treatments at temperatures above 600°C led to a disruption of the macroporous microstructure, to spherical particle formation, and to sintering, as shown by SEM images. Possibly, temperatures higher than 600°C promoted a diffusion of the constituent material of the macroporous walls, causing this material to reassemble into a spherical shape due to energetic factors. The driving force for this behavior could be related to the reduction in the surface energy achieved by the new material microstructure formed by spherical particles that led to a smaller surface area.

Raman spectroscopy and XRD were used to investigate oxide structures after thermal treatments at different temperatures. TiO_2 is known to exist in three distinct crystallographic forms:

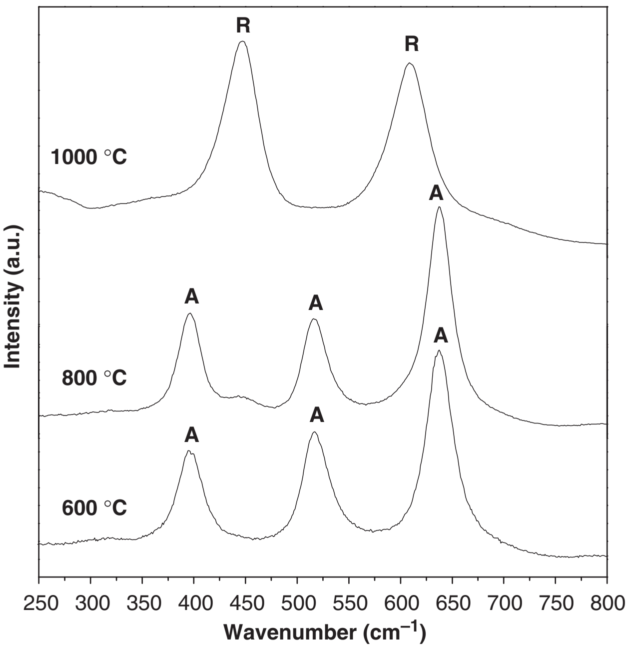

Fig. 7. Raman spectra of the titanium oxide samples thermally treated at 600°, 800°, and 1000°C (A, Anatase peaks; R, Rutile peaks).

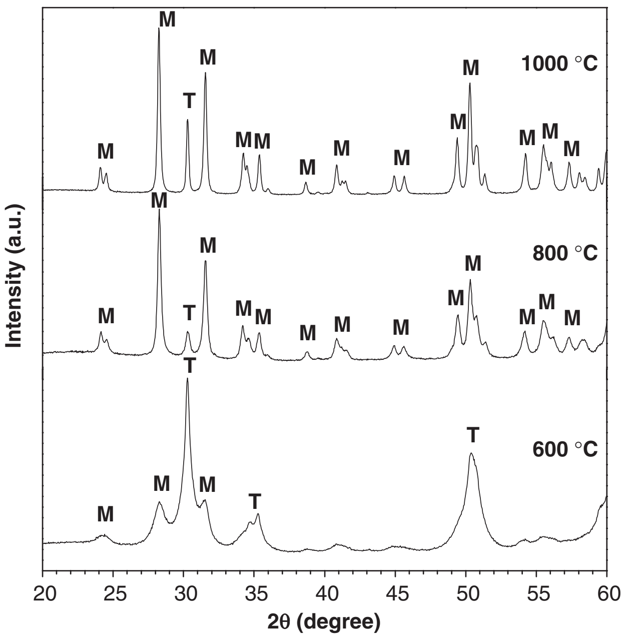

Fig. 9. X-ray diffraction pattern of the zirconium oxide samples thermally treated at 600°, 800°, and 1000°C (T, Tetragonal phase; M, Monoclinic phase).

anatase (tetragonal), brookite (orthorhombic), and rutile (tetragonal). Both anatase and brookite phases can be converted irreversibly into the rutile form when treated at high temperatures. The temperature of the phase transition is sensitive to several factors, such as the experimental procedure used to obtain the TiO_2, reagents, the size of particles, etc. As a general trend, this phase transition begins at around 400°–600°C and it is complete between 800° and 1000°C.[24–28] As shown by the Raman spectroscopy and XRD pattern of TiO_2 samples treated at different temperatures (600°, 800°, and 1000°C), the phase transition from an anatase to a rutile structure was promoted when the temperature was increased from 600° to 1000°C (Figs. 7 and 8, respectively). Raman spectrum for TiO_2 sample heated at 600°C presented peaks near 396, 517, and 637 cm^{-1}, which were related to anatase structure vibrations (Fig. 7). XRD data also corroborated the formation of the anatase phase up to 600°C (Fig. 8). Thermal treatment of the TiO_2 at 800°C led to a higher crystallization of the anatase structure, as can be observed by the presence of well-defined peaks centered at 25.3°, 37.0°, 37.8°, 38.6°, 48.1°, 54.0°, and 55.1° (2θ) in the XRD pattern related to (101), (103), (004), (112), (200), (105), and (211) planes of the anatase phase (Fig. 8).[29] The initial formation of rutile structure from XRD data was also observed at 800°C. When the temperature was increased to 1000°C, the Raman spectrum presented only peaks correlated to the rutile structure at 446 and 610 cm^{-1} (Fig. 7). XRD pattern obtained for this sample presented well-defined peaks centered at 27.5°, 36.2°, 39.3°, 41.3°, 44.2°, 54.5°, and 56.8° (2θ), corresponding to (110), (101), (200), (111), (210), (211), and (220) planes of the rulite structure, which corroborates the complete conversion of the anatase to the rutile phase (Fig. 8).[29]

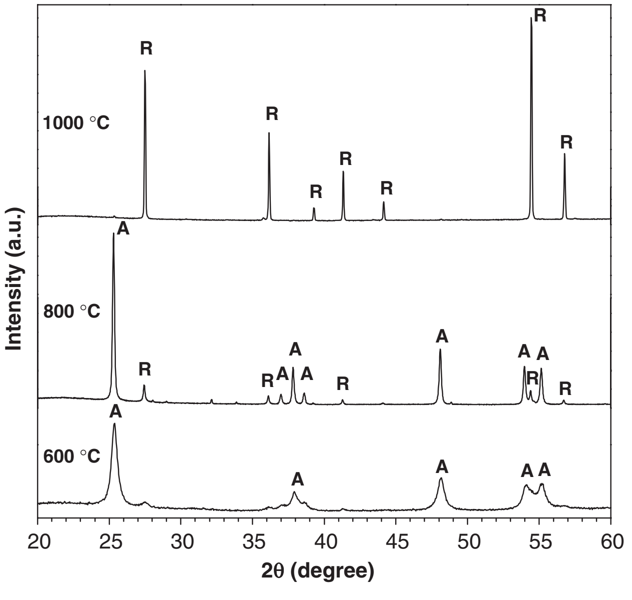

Fig. 8. X-ray diffraction pattern of the titanium oxide samples thermally treated at 600°, 800°, and 1000°C (A, Anatase peaks; R, Rutile peaks).

In the case of ZrO_2, a similar behavior was observed. The material initially formed at 600°C presented a tetragonal structure as the majority phase (Fig. 9). At higher temperatures, a conversion of tetragonal into monoclinic phase took place, resulting in grain growth and macroporous microstructure disruption.[15,16,30]

Subramanian *et al.*[31] observed that the grain growth of TiO_2 prepared by latex templating at temperatures higher than 800°C resulted in macropore collapse. These authors state that the continuous growth of grains, responsible for macroporous microstructure disruption, has not yet been understood completely. Nevertheless, it is known that, in systems where a phase transition occurs through a process involving nuclei formation and further growth, as in the case of TiO_2, there is an increase in the tendency for sintering. This phenomenon is known as the Hedvall effect: during transformation, the breaking and formation of bonds increase the atomic motions, increasing mass diffusion transport. In this way, the nucleation and growth of the rutile phase are responsible for the increase in the diffusion mass, according to the Hedvall effect, favoring macropore collapse and sintering.[32,33]

IV. Conclusions

Different experimental procedures can lead to the formation of macroporous oxides presenting interconnected macropores with a well-defined pore size and controlled three-dimensional ordering from latex templating method. Herein, TiO_2 and ZrO_2 materials were obtained from the latex templating method.

Unusual shrinkage of the pore volume was also observed for the oxide materials after thermal treatment at 600°C. Such a result suggests that different experimental procedures can lead to different shrinkages, allowing the use of templates considerably larger than the final pore size desired.

An investigation of the thermal stability of the oxide macroporous microstructures showed the disruption of macropores at temperatures of 800°C associated with oxide phase transitions. The macroporous microstructure maintained at 600°C makes these materials very interesting for applications in processes at relatively high temperatures.

Acknowledgments

CV acknowledges financial support from the Brazilian Agency FAPESP (99/06491-7). The authors would like to thank LNLS—National Synchrotron Light Laboratory, Brazil—for XRD measurements and LME/LNLS, Campinas, Brazil, for the use of the scanning electron microscope. This is a contribution of PRONEX and Millenium Institute of Complex Materials (IM^2C) programs.

References

[1] A. Imhof and D. J. Pine, "Ordered Macroporous Materials by Emulsion Templating," *Nature*, **389** [6654] 948–51 (1997).

[2] O. D. Velev, T. A. Jede, R. F. Lobo, and A. M. Lenhoff, "Porous Silica Via Colloidal Crystallization," *Nature*, **389** [6650] 447–8 (1997).

[3] B. T. Holland, C. F. Blanford, and A. Stein, "Synthesis of Macroporous Minerals with Highly Ordered Three-Dimensional Arrays of Spheroidal Voids," *Science*, **281** [5376] 538–40 (1998).

[4] J. E. G. J. Wijnhoven and W. L. Vos, "Preparation of Photonic Crystals made of Air Spheres in Titania," *Science*, **281** [5378] 802–4 (1998).

[5] J. D. Joannopoulos, P. R. Villeneuve, and S. Fan, "Photonic Crystals: Putting a New Twist on Light," *Nature*, **386** [6621] 143–9 (1997).

[6] G. Subramania, K. Constant, R. Biswas, M. M. Sigalas, and K. M. Ho, "Optical Photonic Crystals Fabricated from Colloidal Systems," *Appl. Phys. Lett.*, **74** [26] 3933–5 (1999).

[7] A. Richel, N. P. Johnson, and D. W. McComb, "Observation of Bragg Reflection in Photonic Crystals Synthesized from Air Spheres in a Titania Matrix," *Appl. Phys. Lett.*, **76** [14] 1816–8 (2000).

[8] H. Míguez, F. Meseguer, C. López, F. López-Tejeira, and J. Sánchez-Dehesa, "Synthesis and Photonic Bandgap Characterization of Polymer Inverse Opals," *Adv. Mater.*, **13** [6] 393–6 (2001).

[9] Y. Xia, B. Gates, and Z.-Y. Li, "Self-Assembly Approaches to Three-Dimensional Photonic Crystals," *Adv. Mater.*, **13** [6] 409–13 (2001).

[10] D. J. Norris and Y. A. Vlasov, "Chemical Approaches to Three-Dimensional Semiconductor Photonic Crystals," *Adv. Mater.*, **13** [6] 371–6 (2001).

[11] B. T. Holland, C. F. Blanford, T. Do, and A. Stein, "Synthesis of Highly Ordered, Three-Dimensional, Macroporous Structures of Amorphous or Crystalline Inorganic Oxides, Phosphates, and Hybrid Composites," *Chem. Mater.*, **11** [3] 795–805 (1999).

[12] A. Imhof and D. J. Pine, "Uniform Macroporous Ceramics and Plastics by Emulsion Templating," *Adv. Mater.*, **10** [9] 697–700 (1998).

[13] Y. Hotta, P. C. A. Alberius, and L. Bergström, "Coated Polystyrene Particles as Templates for Ordered Macroporous Silica Structures with Controlled Wall Thickness," *J. Mater. Chem.*, **13** [3] 496–501 (2003).

[14] R. C. Schroden, M. Al-Daous, S. Sokolov, B. J. Melde, J. C. Lytle, A. Stein, M. C. Carbajo, J. T. Fernández, and E. Rodríguez, "Hybrid Macroporous Materials for Heavy Metal Ion Adsorption," *J. Mater. Chem.*, **12** [11] 3261–7 (2002).

[15] W. Dong, H. J. Bongard, and F. Marlow, "New Type of Inverse Opals: Titania with Skeleton Structure," *Chem. Mater.*, **15** [2] 568–74 (2003).

[16] M. A. Al-Daous and A. Stein, "Preparation and Catalytic Evaluation of Macroporous Crystalline Sulfated Zirconium Dioxide Templated with Colloidal Crystals," *Chem. Mater.*, **15** [13] 2638–45 (2003).

[17] L. Bechger and W. L. Vos, "Homogeneity of Oxide Air-Sphere Crystals from Millimeter to 100-nm Length Scales: A Probe for Macroporous Photonic Crystal Formation," *Chem. Mater.*, **16** [12] 2425–32 (2004).

[18] Y. N. Kim, S. J. Kim, E. K. Lee, E. O. Chi, N. H. Hur, and C. S. Hong, "Large Magnetoresistance in Three Dimensionally Ordered Macroporous Perovskite Manganites Prepared by a Colloidal Templating Method," *J. Mater. Chem.*, **14** [11] 1774–7 (2004).

[19] Z. Zhou, X. Bao, and X. S. Zhao, "Synthesis, Characterization and Optical Properties of Ordered Macroporous Organosilicas," *Chem. Commum.*, [12] 1376–7 (2004).

[20] J. Bibette, "Depletion Interactions and Fractionated Crystallization for Polydisperse Emulsion Purification," *J. Colloid Interface Sci.*, **147** [2] 474–8 (1991).

[21] V. N. Manoharan, A. Imhof, J. D. Thorne, and D. J. Pine, "Photonic Crystals from Emulsion Templates," *Adv. Mater.*, **13** [6] 447–50 (2001).

[22] H. Míguez, F. Meseguer, C. López, A. Blanco, J. S. Moya, J. Requena, A. Mifsud, and V. Fornés, "Control of the Photonic Crystal Properties of Fcc-Packed Submicrometer SiO_2 Spheres by Sintering," *Adv. Mater.*, **10** [6] 480 (1998).

[23] A. H. Cardoso, C. A. P. Leite, M. E. D. Zaniquelli, and F. Galembeck, "Easy Polymer Latex Self-Assembly and Colloidal Crystal Formation: The Case of Poly[Styrene-co-(2-Hydroxyethyl Methacrylate)]," *Colloids Surf. A*, **144** [1–3] 207–17 (1998).

[24] K. C. Song and S. E. Pratsinis, "Synthesis of Bimodally Porous Titania Powders by Hydrolysis of Titanium Tetraisopropoxide," *J. Mater. Res.*, **15** [11] 2322–9 (2000).

[25] C. C. Wang and J. Y. Ying, "Sol–Gel Synthesis and Hydrothermal Processing of Anatase and Rutile Titania Nanocrystals," *Chem. Mater.*, **11** [11] 3113–20 (1999).

[26] L. J. Alemany, M. A. Banares, E. Pardo, F. Martin-Jimenez, and J. M. Blasco, "Morphological and Structural Characterization of a Titanium Dioxide System," *Mater. Charact.*, **44** [3] 271–5 (2000).

[27] D. Bersani, G. Antonioli, P. P. Lottici, and T. Lopez, "Raman Study of Nanosized Titania Prepared by Sol–Gel Route," *J. Non-Cryst. Solids*, **234**, 175–81 (1998).

[28] U. Balachandran and N. G. Eror, "Raman-Spectra of Titanium-Dioxide," *J. Solid State Chem.*, **42** [3] 276–82 (1982).

[29] Joint Committee on Powder Diffraction Standards (JCPDS), 21-1272 (anatase) and 21-1276 (rutile), 1997.

[30] B. Ksapabutr, E. Gulari, and S. Wongkasemjit, "Preparation of Zirconia Powders by Sol–Gel Route of Sodium Glycozirconate Complex," *Powder Technol.*, **148**, 11 (2004).

[31] G. Subramanian, V. N. Manoharan, J. D. Thorne, and D. J. Pine, "Ordered Macroporous Materials by Colloidal Assembly: A Possible Route to Photonic Bandgap Materials," *Adv. Mater.*, **11** [15] 1261 (1999).

[32] J. Nair, P. Nair, F. Mizukami, Y. Oosawa, and T. Okubo, "Microstructure and Phase Transformation Behavior of Doped Nanostructured Titania," *Mater. Res. Bull.*, **34** [8] 1275–90 (1999).

[33] K.-N. P. Kumar, "Porous Nanocomposites as Catalyst Supports. 1. 2nd-Phase Stabilization, Thermal-Stability and Anatase-to-Rutile Transformation in Titania-Alumina Nanocomposites," *Appl. Catal. A*, **119** [1] 163–83. □